

Preliminary Estimation of Particle Dry Deposition Fluxes along Coastal Area of Jeju Island

Ki-Ho Lee and Chul-Goo Hu

Department of Environmental Engineering, Cheju National University

(Manuscript received on March 5, 2001)

This work employs two models to quantify the size-segregated dry deposition fluxes of particle-bound NO_3^- , NH_4^+ , and SO_4^{2-} along the coastal area of Jeju Island based on the chemical composition data of aerosol collected during the springtime of 1995.

The two approaches produced fairly comparable results, despite the feature differences between the two models. The modelling results obtained indicated that the mean dry deposition velocity was around 0.4 cm s^{-1} for NO_3^- , 0.2 cm s^{-1} for NH_4^+ , and 0.3 cm s^{-1} for SO_4^{2-} , and the dry deposition flux varied between $371 \sim 1368 \mu\text{gm}^{-2}\text{day}^{-1}$ for nitrate, $28 \sim 625 \mu\text{gm}^{-2}\text{day}^{-1}$ for ammonium, and $957 \sim 6088 \mu\text{gm}^{-2}\text{day}^{-1}$ for sulfate. Although difficulties in collecting giant and/or fine particles limited the understanding of the mass size distribution of particles and thus the ability to refine estimates of the dry deposition flux for the particulate matter, both models were still able to offer sufficient realism to explain the features of the available data collected from the coastal area of Jeju Island.

Key words : particle deposition, model, sulfate, ammonium, nitrate, East China Sea

1. Introduction

It is well known that in addition to wet deposition, the dry deposition of particles is also responsible for delivering atmospheric loads of various trace species, such as SO_4^{2-} , NO_3^- , and NH_4^+ , base cations and heavy metals to ecosystems. The deposition of particles containing SO_4^{2-} , NO_3^- , and NH_4^+ in natural bodies of water contributes to the potential acidification and eutrophication of ecosystems (Ruijgrok et al., 1995). The eutrophication of water bodies can be enhanced by excess nutrient inputs, while toxic species deposition can harm aquatic life or make plants and animals harmful to those higher up in the food chain. The elevated levels of toxic and acidic species in the Great Lakes has been partially attributed to the atmospheric dry deposition of pollutants (Pirrone et al, 1995). Gatz (1975) estimated that dry deposition accounts for 50% of the total atmospheric deposition of several trace species in Lake Michigan. Wu et al.(1994) found dry deposition to be responsible for approximately 80 % of the total atmospheric flux

of Al and Fe, and 50 % of the total atmospheric flux of As, Cr, Cu and Ni in the Chesapeake Bay. Numerous recent studies have indicated that, based on the total atmospheric deposition, about 30 % of sulfur species and 30~70 % of nitrogen species are a result of dry deposition. These significant fractions suggest that about one half of the total acid deposition occurs in the absence of rainfall.

Currently, several investigators have suggested that the vicinity of Asian aerosol sources and Chinese aerosol sources may induce higher dry deposition velocities than over other remote oceanic regions. Consequently, there are growing the concern over the pollution of the coastal and shelf systems of the East China Sea. As such, the coastal area around Jeju Island is believed to be subject to the deposition of Asian aerosol and anthropogenic air pollutants as it lies in close proximity to China and receives polluted air masses from the heavily industrialized areas in the eastern part of the Chinese mainland. Despite the importance of these situations, current knowledge is still insufficient to provide an adequate

assessment of the dry deposition of particulate matter over North-East Asia.

In general, dry deposition implies the transfer of material in a gas or solid phase. A air-water dry deposition flux can be calculated from the product of a concentration term and the dry deposition velocity. However, concentrations are not readily available for large areas over the sea, and the dry deposition velocity varies with the particle size (Rojas et al., 1993). Accordingly, mathematical models have been introduced as an alternative tool to estimate a dry deposition flux. A number of models which describe the dry deposition of particles exist. In general, these models fall into two categories: process-oriented models and bulk-resistance models (Ruijgrok et al., 1995). However, the evaluation of the results of both model types using measured data has been relatively poor, especially, in Korea. Yet such an evaluation is urgently needed in order to more accurately assess the contribution of dry deposition fluxes of acidifying aerosols to the total load received by the water bodies around Jeju Island.

In this paper, the preliminary dry deposition flux of particle bound soluble constituents along the coastal area of Jeju Island is estimated using two process-oriented models. This modelling effort is undertaken to enable a better understanding and provide a basis for assessing the input related to the dry deposition of acidifying aerosols in the coastal area of Jeju Island, Korea.

2. Computation of Dry Deposition Velocity

Direct dry deposition measurements are difficult to make or apply reliably, and often require extensive and expensive instrumentation. To make up for this deficiency, models have been developed that infer removal rates based on a knowledge of micrometeorological parameters. The dry deposition process for aerosol particles is primarily the sum of several physical transfer processes, including gravitational settling, turbulent diffusion, and impaction. Therefore, the dry deposition flux of material to the water surface is calculated from the product of the atmospheric concentration and the dry deposition velocity. The dry deposition velocity of aerosol is strongly dependent on the particle size and meteorological factors, primarily

wind speed and humidity.

One of the most widely used theoretical approaches to the dry deposition of particles is that developed by Slinn and Slinn (1980), which is employed in the current study. Its applications have also been reported by Dulac et al. (1989), Steiger et al. (1989), and Baeyens et al. (1990). In this model, the atmosphere below 10 m is conceptually divided into two layers. In the upper layer, the transport of a particle is mainly governed by atmospheric turbulence and gravitational settling, while in the lower layer close to the air-sea interface, Brownian diffusion and particle growth due to hygroscopicity are predominant. Therefore, atmospheric turbulence is assumed to have a negligible direct influence on particle transport in the lower layer. However, it should be pointed out that in this study, corrections for particle scavenging due to wave breaking, spray formation, and atmospheric stability are not introduced. The equations related to this model are reported elsewhere (Dulac et al., 1989; Arimoto and Duce, 1986; Slinn and Slinn, 1980).

The other model used in this study is based on the work of Pryor et al. (1999). The model was originally developed by Williams (1982) and further developed by Hummelshoj et al. (1992). In this model, the method for determining the transfer velocity across the laminar surface layer incorporates the effects of the enhancement of the transfer due to bubble burst as well as diffusional transfer and particle growth due to hygroscopicity. The particle deposition velocity is basically given as

$$v_d = \frac{(v_h + v_{g,d})(v_\delta + v_{g,w})}{v_h + v_\delta + v_{g,d}} \quad (1)$$

where v_h is the transfer velocity in the layer dominated by turbulent transfer, v_g is the transfer velocity due to gravitational settling, and the additional subscripts d and w mean dry and wet states, respectively. v_δ is the transfer velocity across the laminar surface layer. The procedures for computing these transfer velocities are basically the same as those presented by Pryor et al. (1999), except for certain relations. Only the exceptions are described below.

To predict the dry deposition velocity from this model, estimates of both the aerodynamic surface

roughness height(z_0) and the air friction velocity (u_*) are needed. The friction velocity is a convenient and useful measure of the turbulent intensity. For cases where the wind speed is measured directly, it is possible to estimate u_* from Equation (2) for typical conditions at sea(Slenn, et al., 1978).

$$u_* = 0.037u \tag{2}$$

where u is the mean wind speed.

The surface roughness length is calculated using the Charnock equation(given in Table 2). The stability correction is determined based on the Monin-Obukhov stability parameter(z/L) and is calculated as shown in the Appendix published by Pryor et al.(1999). In this work, z/L is calculated by Equation (3) as given by Williams(1982).

$$z/L \approx g(T_a - T_w)z \ln(z/z_0)/T_a u^2 \tag{3}$$

where T_a and T_w are the air and water temperatures, respectively.

The magnitude of the dry deposition velocity is a function of Brownian and eddy diffusivities and gravity settling. For particle diameters larger than about 1 μm , the deposition velocities increase because of an increase in the eddy diffusion and gravitational settling. For larger particles, the deposition velocities approach their respective gravitational settling velocity. For very small particles below 0.1 μm , the deposition velocity increases with a decreasing particle diameter because of Brownian diffusion. The Brownian diffusivity of the particle is given by Equation (4) (Dulac et al., 1989 ; Arimoto and Duce, 1986; Williams, 1982).

$$B_d = (2.38 \times 10^{-7}/d_w) (1+0.163/d_w + 0.0548 \exp(-6.66d_w)/d_w) \tag{4}$$

where d_w is the particle diameter in equilibrium with the higher near-surface humidity. Because B_d

is calculated for the near-surface laminar layer, d_w is used in this equation (4), which is calculated using the relation given by Fitzgerald (1975). In the current work, the dry state particle density was assumed to be 2.1 and the wet state particle density 1.1. The parameterization applied is described in more detail by Pryor et al. (1999).

These particular models were selected based on a review of currently available models which covered all relevant removal processes. The main features of the models considered in this study and the specific parameters they utilize are summarized in Tables 1 and 2, respectively.

3. Chemical Analysis

A map showing the location where the sampling was carried out is given in Fig. 1. The field sampling started in 10 March, 1995 and lasted for eight weeks along the west coast of Jeju Island(33° 17' N, 126° 10' E). The sampling site had an unimpeded view of the sea and was about 10 m from the shore at an altitude of 70 m above sea level. Size segregated aerosol samples were obtained for seven days using an eight-stage multi-orifice cascade impactor at an operational flow rate of $29 \pm 1 \text{ l min}^{-1}$. The particle sizes deposited at each stage were as follows from stage 1 to 8 : 0.43~0.65 μm , 0.65~1.1 μm , 1.1~2.1 μm , 2.1~3.3 μm , 3.3~4.7 μm , 4.7~7.0 μm , 7.0~11 μm , and above 11 μm . A backup filter collected the smallest particles. In order to analyze the water-soluble ionic components the aerosol deposited on each filter was extracted ultrasonically with deionized water (17~18 M Ω) and 0.5 ml of ethanol. The extracts were analyzed using an ion-chromatograph(IC) to determine the mass concentrations of the major anions and by an atomic absorption spectrophotometer for the cations, except for NH_4^+ , which

Table 1. Characteristic feature of each model describing the dry deposition of particle on water surface

Model	Processes included in the model								
	Stability	Turbulent transport	Sedimentation	Impaction	Interception	Brownian diffusion	Rebound	Hygroscopic growth	Capture by waves
Slenn & Slenn(1980)	-	+	+	+	+	+	-	+	-
Pryor et al(1999)	+	+	+	+	+	+	-	+	+

- : not included

Table 2. Specified parameters introduced in two models

Parameter	Specified parameter	
	model 1	model 2
Size of Particle (d_d)	8 classes	same as model 1
Wind speed (u)	use the measured data(hourly)	same as model 1
Relative humidity	use the measured data(hourly)	same as model 1
Sea surface temperature	use monthly mean data	same as model 1
Stability correction($\Psi_h(z/L)$)	use the eq. (3)	not considered
Frictional velocity(u_*)	use the eq. (2)	same as model 1
Surface roughness length(z_0)	use the Charnock eq. : (au_*^2/g with $a=0.0185$)	not considered
Particle density :		same as model 1
dry state	2.1	
wet state	1.1	
Turbulent transfer velocity(v_h)	$\kappa u_* / [\ln(z/z_0) + \Psi_h(z/L)]$	no stability correction
Gravitational settling velocity	by Stokes law	same as model 1
Brownian diffusivity	use the eq. (4)	same as model 1
Hygroscopic growth of particle	by Fitzgerald relation	same as model 1
Bubble burst activity :	$u_*^2 / u + \text{Eff}(2 \pi r_{\text{drop}}^2)(2z_{\text{drop}})q_{\text{drop}} / \alpha$	not considered
- capture efficiency of particles by spray drops (Eff)	0.5	
- average radius of the spray drop(r_{drop})	0.1	
- flux of spray drop from surface(q_{drop})	$5(100 \alpha)$	
- sea surface area covered by whitecaps(α)	$1.7 \times 10^{-6} u^{3.75}$	

was analyzed using the Indophenol method. The quantifiable species were : Nitrate(NO_3^-), sulfate(SO_4^{2-}), chloride(Cl^-), sodium(Na^+), ammonium(NH_4^+), calcium(Ca^{2+}), potassium(K^+), and magnesium(Mg^{2+}).

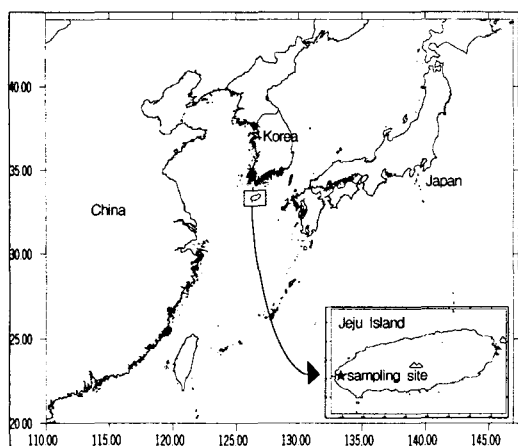


Fig. 1. Location of Jeju Island and sampling site.

Meteorological data were gathered concurrently at the National Meteorological Observatory Station located at the sampling site, from which the current study considered the hourly averaged data. The sea surface temperature was considered based on the monthly mean value because of the difficulty involved with continuous measurement. In modeling, the deposition velocity for each particle size was calculated relative to the hourly averaged meteorological data, then the weekly averaged deposition velocity was computed for each particle size and sampling time.

4. Results and Discussion

4.1. Chemical composition

Figure 2 shows the bulk composition of the ions measured on the substrates for each sample. As shown in Fig. 2, the sample to sample variability in the measured ion concentrations was small except for sample 1. Sample 1, during which an

Asian dust-storm was observed(from 12 to 13, March), exhibited the highest overall concentrations, although the ion concentrations were relatively constant towards the end of the measurement period. It has been previously reported that the concentrations of sulfate and nitrate in Japan during Asian dust-storm periods are 3~8 times higher than during non-storm periods(Zhang and Iwasaka, 1999). Okada et al.(1990) also reported that individual Asian dust particles collected over the Japanese islands sometimes included an internal mixture of water-soluble and insoluble materials, and the water-soluble material mainly contained S and Ca.

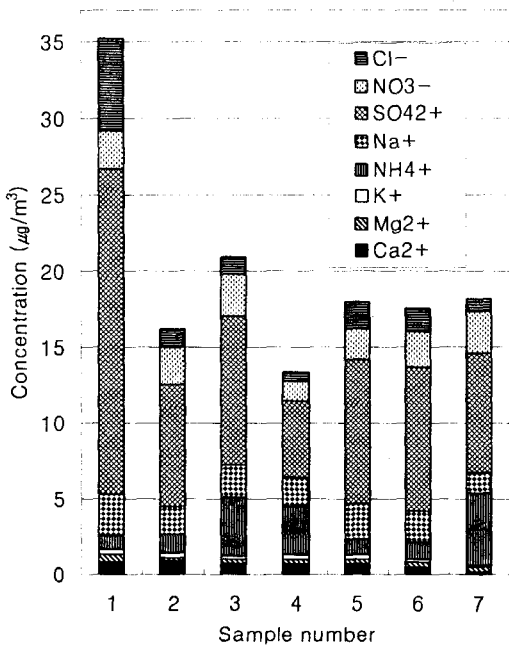


Fig. 2. Bulk ion composition for each sample.

The chemical analysis performed on the filters did not provide an estimate of the total mass since the particle-bound water and mass attributable to the organics and other components were not analyzed. As shown in Fig. 2, the mass concentrations of Na⁺ and Cl⁻ in the particles were relatively low despite the coastal location. It is known that the heterogeneous chemistry of nitric acid on sodium chloride particles can yield particle sodium nitrate and lead to the volatilization of hydrochloric acid vapor. Evidence of this process is presented in Fig. 3 where the molar ratio of

Na⁺ to Cl⁻ for each stage was relatively high.

Figure 4 shows the ion balances for each stage and sample, where the ion balance indicated a ratio of almost unity for cations and anions.

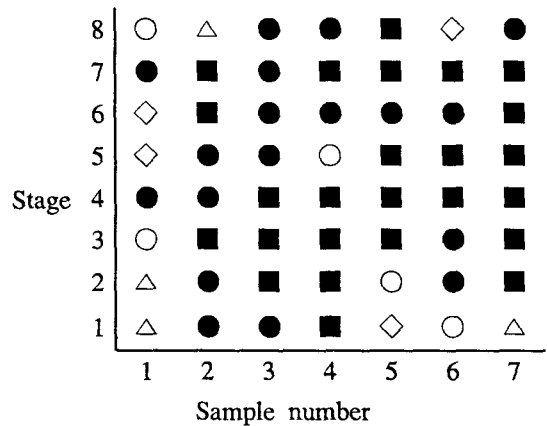


Fig. 3. Molar ratio of Na⁺/Cl⁻ by sample(x-axis) and stage(y-axis).

(■ : >3.0, ● : 1.2-3.0, ◇ : 0.8-1.2, △ : 0.8-0.5, ○ : 0.0-0.5).

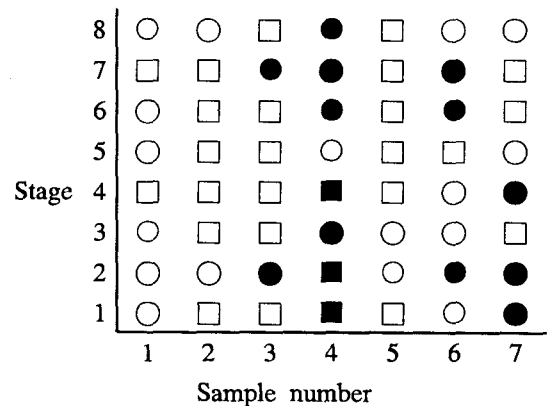


Fig. 4. Ion balance for each sample and stage. The molar ratio was

$$\frac{Na^+ + NH_4^+ + K^+ + 2Mg^{2+} + 2Ca^{2+}}{Cl^- + NO_3^- + 2SO_4^{2-}}$$

(■ : 2.0-4.0, ● : 1.3-2.0, □ : 0.7-1.3, ○ : 0.1-0.7)

4.2. Dry deposition velocities

Hereafter, model 1 and model 2 refer to the models of Pryor et al.(1999) and Slinn and Slinn (1980), respectively

Table 3 compares the average dry deposition

Table 3. Average dry deposition velocities computed by two models for NO_3^- , NH_4^+ and SO_4^{2-} contained in airborne particles sampled at the western coastal area of Jeju Island

Approach	Average dry deposition velocities ($\text{cm} \cdot \text{s}^{-1}$)		
	NO_3^-	NH_4^+	SO_4^{2-}
Model 1	0.398 ± 0.124	0.210 ± 0.179	0.2799 ± 0.066
Model 2	0.402 ± 0.077	0.198 ± 0.184	0.3086 ± 0.052

velocities resulting from the two models for NO_3^- , NH_4^+ , and SO_4^{2-} measured for the coastal area of Jeju Island. As seen from this table, the two approaches produced fairly comparable results despite the inclusion of atmospheric stability and parameters for capture by wave, i.e. bubble burst activity, in model 1. Although Arimoto and Duce (1986) reported that the Williams model, which provides the fundamentals in model 1, predicts higher deposition velocities for submicrometer particles than the Slinn and Slinn model(model 2), the values for the average dry deposition velocities predicted by model 1 and model 2 were close in the current study. The reason for this was due to the size distribution of the atmospheric particulate matter. The dry deposition velocities were mass weighted, i.e., the deposition velocities corresponding to a certain particle size were scaled based on the ratio of the aerosol mass accounted for that particle size.

Therefore, the modelling results obtained here indicated a mean dry deposition velocity of around 0.4 cm s^{-1} for NO_3^- , 0.2 cm s^{-1} for NH_4^+ , and 0.3 cm s^{-1} for SO_4^{2-} .

4.3. Dry deposition fluxes

Figures 5 and 6 show a summation of the dry deposition fluxes for all the particle sizes and the classified dry deposition fluxes of NO_3^- , NH_4^+ , and SO_4^{2-} by sample and particle diameter(stage). As shown in Figs. 5 and 6, the total deposition flux varied by over an order of magnitude for the different sampling periods and the contribution of the different particle sizes was also highly variable. The values for the dry deposition fluxes predicted by both models were substantially the same, plus the fluctuation patterns observed during the

sampling period were also the same. For NO_3^- , the dry deposition flux ranged between $371 \sim 1368 \mu\text{g m}^{-2} \text{ day}^{-1}$ with model 1 and $484 \sim 1161 \mu\text{g m}^{-2} \text{ day}^{-1}$ with model 2, and was dominated by the deposition in particles with diameters greater than $2.1 \mu\text{m}$ (corresponding to stage 3), as shown in Fig. 6(a). For SO_4^{2-} , the dry deposition flux ranged between $957 \sim 5951 \mu\text{g m}^{-2} \text{ day}^{-1}$ with model 1 and $1268 \sim 6088 \mu\text{g m}^{-2} \text{ day}^{-1}$ with model 2, and the fluctuation pattern was similar to that for NO_3^- . The dry deposition flux of SO_4^{2-} was also dominated by a large particle deposition, as shown in Fig. 6(c). Zhou et al.(1996) reported that sea salt and sulfur are accumulated on dust particles during the transport from China to Japan. Nishikawa et al. (1991) reported that the NO_3^- and SO_4^{2-} in the coarse fraction of Asian dust aerosol are related to soil particles originating from a Chinese arid area. This observation indicates the potential importance of heterogeneous chemistry on sea salt particles in determining particle NO_3^- and SO_4^{2-} dry depositions(Pryor et al., 1999). Pryor et al.(1999) reported that ammonium exhibits a bimodal distribution and hence the deposition flux of NH_4^+ is strongly dependent on the contribution from accumulation mode(diameter $0.11 \sim 0.5 \mu\text{m}$) par-

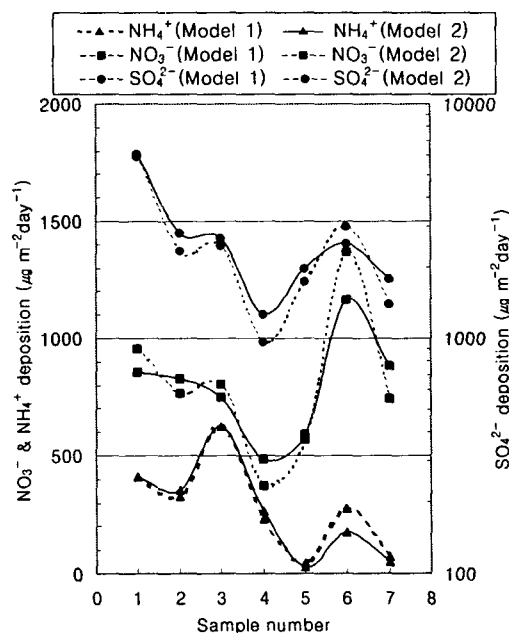
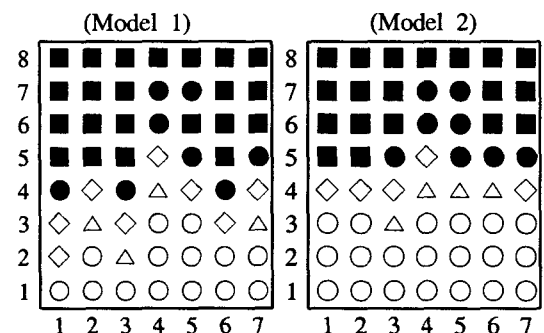
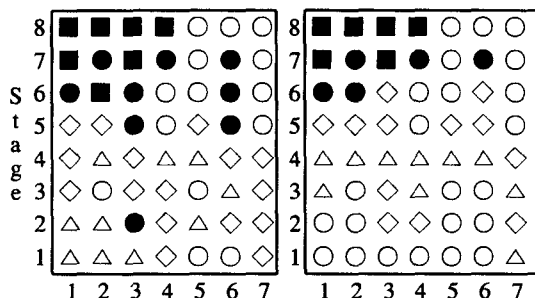


Fig. 5. Variation of dry deposition fluxes for all particle sizes by sample.



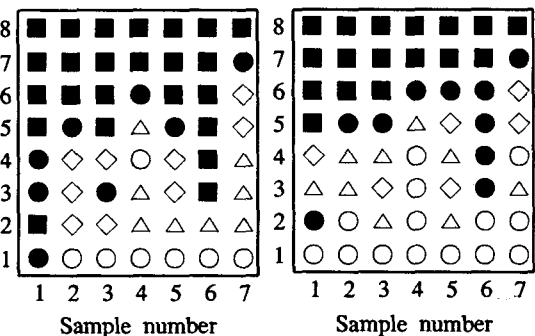
(a) Nitrate

○ : 0.-10. △ : 10.-20.
◇ : 20.-50. ● : 50.-100. ■ : >100.



(b) Ammonium

○ : 0.- 5. △ : 5.-10. ◇ : 10.-25.
● : 25.-50. ■ : >50.



(c) Sulfate

○ : 0.- 25. △ : 25.-50. ◇ : 50.-100.
● : 100.-200. ■ : >200.

Fig. 6. Dry deposition fluxes of (a) NO_3^- , (b) NH_4^+ , and (c) SO_4^{2-} by sample and stage.

ticles and coarse particles (diameter > 1.9 μm). However, Fig. 6(b) does not show an explicit dependency of the ammonium deposition on the particle distribution because the method used for particle segregation (especially in submicrometer particles) was different from that used by Pryor

et al. (1999). In this work, the difficulty in separating the fine particles limited the understanding of the particle size distribution. Yet, the dependency of the dry deposition fluxes on the particle size can be clearly confirmed in Fig. 7.

In Fig. 7, the dry deposition flux and atmospheric mass are given for each size fraction. As a result, the dominant contribution of the large particle fraction to the overall dry deposition flux was evident, even though it may have only contributed a small fraction to the total mass. The same pattern was also observed in previous literature on various elements such as Al, Pb, Cd, Cu, Cr, Ni, and Zn (Injuk et al., 1998; Dulac et al., 1989), due to the large deposition velocities associated with larger particles. Injuk et al. (1998) also pointed out that the uncertainty in a dry deposition flux strongly

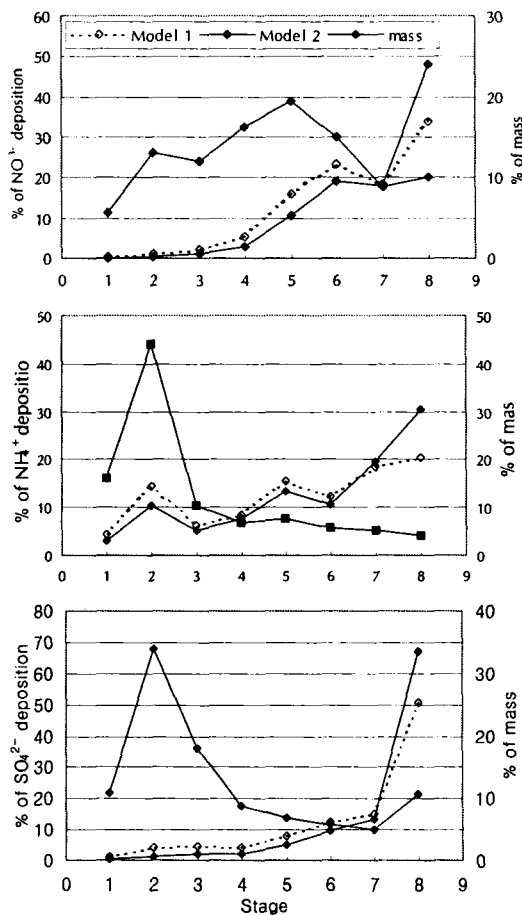


Fig. 7. Relative contribution of each size fraction to atmospheric mass and dry deposition flux.

depends on the accuracy of the aerosol size distribution, especially the large size fraction. Many researchers (Ottley and Harison, 1993; Dulac et al., 1989; Steiger et al., 1989) have already demonstrated the dominant contribution of the large particle fraction to the overall dry deposition flux. For the case of NH_4^+ shown in Fig. 6(b), the contribution of the fine particle fraction to the overall dry deposition flux was more significant than the cases of NO_3^- and SO_4^{2-} . Pryor et al. (1999) also reported that the dry deposition flux of NO_3^- is dominated by the deposition in particles with diameters greater than $2 \mu\text{m}$, whereas an NH_4^+ dry deposition flux is dominated by particles in two modes: $0.1 \sim 0.3 \mu\text{m}$ and greater than $3 \mu\text{m}$.

Table 4 shows the dry deposition fluxes calculated from the average dry deposition velocities. The results of the modelling presented here suggest that dry deposition fluxes including sulfur and nitrogen in the particles vary over a large range even during a relatively short period. Table 4 also shows values of dry deposition fluxes that are substantially larger than those reported in previous literature (Morales et al., 1998; Pryor et al., 1999). Since the current study does not present any definitive direct measurements of particle deposition velocities, the level of uncertainty in the dry deposition velocities is still unclear. However, Ruijgrok et al. (1995) suggested that for SO_4^{2-} , and in some cases NO_3^- , the effect of local sources and the resulting concentration variations in deposition are only a minor concern, whereas for NH_4^+ and alkaline particles, local variations in concentration may be important. Accordingly, it would seem reasonable to postulate that the relative importance of sulfate and nitrate in spring-time along the coastal area of Jeju Island is based on the Asian dust storms from the Asian continent to the North Pacific Ocean (Nishikawa et al., 1991;

Table 4. Dry deposition fluxes of NO_3^- , NH_4^+ and SO_4^{2-} contained in airborne particles sampled at the western coastal area of Jeju Island

Approach	Dry deposition fluxes ($\mu\text{g m}^{-2}\text{day}^{-1}$)		
	NO_3^-	NH_4^+	SO_4^{2-}
Model 1	795.6 ± 313.3	282.8 ± 198.0	2554.2 ± 1650.1
Model 2	791.8 ± 218.9	272.4 ± 212.2	2736.9 ± 1575.8

Zhang and Iwasaka, 1999). Although large uncertainties still exist, the models presented here were able to contain sufficient realism to explain the features of available data collected from the coastal area of Jeju Island.

5. Conclusions and Recommendations

This work employed two models to calculate the size-segregated dry deposition fluxes of particle-bound nitrogen and sulfur compounds in the coastal area of Jeju Island based on the chemical composition data of aerosol collected during the springtime of 1995.

The two approaches produced fairly comparable results, despite the feature differences between the two models. The modelling results obtained indicated that the mean dry deposition velocity was around 0.4 cm s^{-1} for NO_3^- , 0.2 cm s^{-1} for NH_4^+ , and 0.3 cm s^{-1} for SO_4^{2-} , and the dry deposition flux varied between $371 \sim 1368 \mu\text{g m}^{-2}\text{day}^{-1}$ for nitrate, $28 \sim 625 \mu\text{g m}^{-2}\text{day}^{-1}$ for ammonium, and $957 \sim 6088 \mu\text{g m}^{-2}\text{day}^{-1}$ for sulfate. The dry deposition fluxes of NO_3^- , NH_4^+ , and SO_4^{2-} on the west coast of Jeju Island were substantially larger than those reported in previous literature due to the role of the Asian dust storms from the Asian continent during springtime in North-East Asia. However, since the parameterization for dry deposition processes is still highly uncertain, the reality of these values and the actual level of uncertainty in the dry deposition velocities are still unclear. Given the importance of understanding and predicting mineral loads in coastal water, further research is required to quantify the total loads and mineral deposition pathways.

Acknowledgements

This work was supported by a grant from the Cheju National University Development Foundation in the program year of 2000. The authors would like to thank the Marine Research Institute of Cheju National University for its financial support. Sincere thanks also go to the three anonymous reviewers.

References

- [1] Arimoto, R. and R. A. Duce, 1996, *J.*

- Geophys. Res.* 91, 2787~2792.
- [2] Baeyens, W., F. Dehairs and H. De-deurwaerder, 1990, *Atmos. Environ.* 24A, 1693~1703.
- [3] Dulac, F., P. Buat-Menard, U. Ezat, S. Melk and G. Bergametti, 1989, *Tellus* 41B, 362~378.
- [4] Fitzgerald, J.W., 1975, *J. Appl. Meteor.* 14, 1044~1049.
- [5] Gatz, D., 1975, *Water, Air, and Soil Pollution* 5, 239~251.
- [6] Hummelshoj, P., N. O. Jensen and S. E. Larsen, 1992, Particle dry deposition to a sea surface, In : S. E. Schwartz and W. G. N. Slinn(eds) : Precipitation scavenging and atmosphere-surface exchange processes, Hemisphere Publ., Washington DC, 829~840.
- [7] Injuk, J., R. Van Grieku and G. De Leeuw, 1998, *Atmos. Environ.* 32, 3011~3025.
- [8] Morales, J. A., C. Bifano and A. Escalona, 1998, *Atmos. Environ.* 32, 3051~3058.
- [9] Nishikawa, M., S. kanamori, N. Kanamori and T. Mizoguchi, 1991, Environmental significance of Kosu aerosol(yellow sand dust) collected in Japan, Proc. of the 2nd IUAPPA Regional Conference on Air Pollution, Sep. 4 to 6, Seoul Korea, pp.35~41.
- [10] Okata, K., H. Naruse, T. Tanaka, O. Nemoto, Y. Iwasaka, P. Wu, A. Ono, R. Duce. M.Uematsu and J. Merrill, 1990, *Atmos. Environ.* 24, 1369~1378.
- [11] Ottley, C. J. and R. M. Harrison, 1993, *Atmos. Environ.* 27A, 685~695.
- [12] Pirrone, N., G. J. Keeler, T. M. Holsen, 1995, *Environ. Sci. Technol.* 29, 2112~2122.
- [13] Pryor, S. C., R. J. Barthelmie, L. L. S. Geernaert, T. Ellermann, and K. D. Perry, 1999, *Atmos. Environ.* 33, 2045~2058.
- [14] Rojas, C. M., J. Injuk, R. E. Van Grieken and R. W. Laane, 1993, *Atmos. Environ.* 27A, 251~259.
- [15] Ruijgrok, C. I. Davidso and K. W. Nicholson, 1995, *Tellus* 47B, 587~601.
- [16] Slinn, W. G. N., L. Hasse, B. B. Hicks, A.W. Hogan, D. Lal, P. S. Liss, K. O. Minnich, G. A. Sehmel and O. Vittori, 1978, *Atmos. Environ.* 12, 2055~2087.
- [17] Slinn, S. A. and W. G. N. Slinn, 1980, *Atmos. Environ.* 14, 1013~1016.
- [18] Steiger, M., M. Schulz, M. Schwikowski, K. Naumann and W. Dannecker, 1989, *J. Aerosol Sci.* 20, 1229~1232.
- [19] Williams, R. M., 1982, *Atmos. Environ.* 16, 1933~1938.
- [20] Wu, Z. Y., M. Han, Z. C. Lin and H. M. Ondov, 1994, *Atmos. Environ.* 28, 1471~1486.
- [21] Zhang, D. and Y. Iwasaka, 1999, *Atmos. Environ.* 33, 3213~3223.
- [22] Zhou, M., K. Okada, F. Qian, P. Wu, L. Su, B. Casareto, T. Shimohura, 1996, *Atmos. Environ.* 40, 19~31.